NUMERICAL STUDY OF CHORD END DISTANCE EFFECT ON RHS X-CONNECTIONS

XIAO-DING BU[1] and JEFFREY A. PACKER[1]

[1]*Department of Civil & Mineral Engineering, University of Toronto, Ontario M5S 1A4, Canada*

E-mail: deanx.bu@mail.utoronto.ca; jeffrey.packer@utoronto.ca

The proximity of a welded hollow structural section connection to the end of the chord is known to have an effect on the connection strength, particularly if the chord member has an open end. In order to achieve the capacity of a connection remote from an open chord end, minimum end distances are being proposed for codes and standards (such as prEN 1993-1-8, AISC 360 and ISO 14346). While only limited experiments have been done on this topic for rectangular hollow sections (RHS), this paper provides a broader numerical study of such RHS connections. Non-linear finite element models, which are validated against the former laboratory experiments, are used to generate a database of 132 numerical tests covering a wide range of geometric connection parameters. Based on the study, a single value for the required chord end distance, to achieve full connection strength, is given as a lower bound to cover all limit states under branch compression. For connections with an end distance smaller than the requirement, a strength reduction is proposed as a function of the branch-to-chord width ratio.

Keywords: Rectangular hollow sections, connections, joints, chord length, open-end proximity, finite element analysis.

1 Introduction

Rectangular hollow sections are widely used in the steel construction industry, especially in trusses, frames and many other applications. In many cases, the design of the connections governs the strength of the structure. In current hollow section design recommendations, it is assumed that the RHS connections are symmetric about the chord centerline and that the chord member has sufficient continuity beyond the connection region. This type of connection is referred to herein as a "traditional connection". Such situations are occasionally violated, and none of the contemporary recommendations deal adequately with "irregular" connections where branches are near the end of an open-ended RHS chord member (termed a "longitudinally offset connection"). This connection type is illustrated in Figure 1.

A proposed revision to EN 1993-1-8 (CEN 2010) in prEN 1993-1-8 (2018) includes a minimum end distance, e_{min}, which is the larger of: $(2\gamma/10)b_0$ (or h_0 if $h_0 > b_0$), and $2.5b_0$ (or h_0 if $h_0 > b_0$). This applies to all RHS connection types, where $2\gamma = b_0/t_0$ is the chord slenderness, b_0 is the chord width, h_0 is the chord height, and t_0 is the chord thickness. This recommendation was extrapolated from research on end-distance effects on circular hollow section (CHS) connection capacity. For simplicity, e_{min} was conservatively taken as the clear distance from the nearest branch to the open chord end.

AISC 360-16 Chapter K (AISC 2016) includes a required minimum end distance of $e_{min} = b_0\sqrt{1-\beta}$ (where $\beta = b_1/b_0$ is the branch-to-chord width ratio), in order to achieve full connection

Proceedings of the 17th International Symposium on Tubular Structures.
Editors: X.D. Qian and Y.S. Choo

Published by Research Publishing, Singapore.
ISBN: 978-981-11-0745-0; doi:10.3850/978-981-11-0745-0_048-cd

strength, for T-, Y- and X-connections. This is based on yield line mechanisms in the RHS chord connecting face, supported by laboratory tests (Fan and Packer 2017). This rule, however, presumes that the chord plastification limit state controls. The Commentary to AISC 360-16 (AISC 2016) Chapter K suggests that, if the connection is close to a chord open end, the full connection strength predicted by regular design rules may be reduced by 50%; alternatively, the full connection strength can be re-gained by capping the end of the chord.

Recent research (Fan and Packer 2017) has investigated the behavior and failure modes of T-shaped RHS X-connections with the branch close to a chord end, such as shown in Fig. 1, through experiments. This paper presents a non-linear finite element (FE) study with models validated against these prior experiments in which the branch was loaded in axial compression. The FE modeling is then extended by varying the connection end distances to numerically study the effect of the end distance on the connection strength over a wider parameter range.

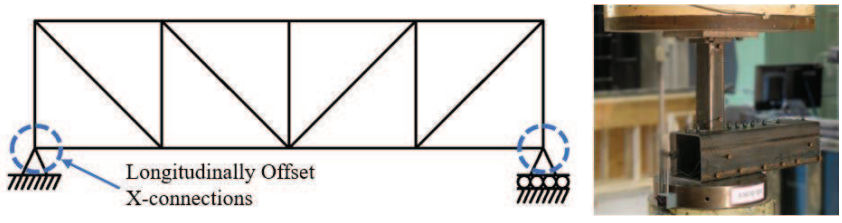

Figure 1. End connection in an RHS Pratt truss and test setup by Fan and Packer (2017)

2 Experimental Database

Experimental research by Fan and Packer (2017) included 16 test specimens, all of which were fabricated with only one branch member welded to each chord member, in a T-shape (see Fig. 1). All connections were tested to failure in a quasi-static manner in branch axial compression, using a universal testing machine, where a load was applied to the top of the branch and the opposite face of the chord was supported on a pedestal. The validation of FE models for four representative laboratory tests is presented herein. The member geometric properties used in the FE models and the selected connections are summarized in Tables 1 and 2, respectively.

Table 1. Measured RHS member dimensions by Fan and Packer (2017)

Designation [mm]	Member	Width and Height [mm]	Wall Thickness [mm]	Corner Radius	
				Outer r_o [mm]	Inner r_i [mm]
HSS203x203x9.53	Chord	203.1	8.9	23.8	15.0
HSS102x102x9.53	Branch-1	101.7	8.7	18.6	9.7
HSS203x203x12.7	Branch-2	204.0	11.7	32.7	21.0

Table 2. Test specimens by Fan and Packer (2017) modeled in this study

Specimen No.	Specimen Identification	Member Combination	Nominal β	End Distance e [mm]
1	X-0.5-21-25O	Chord + Branch-1	0.5	25
2 (control)	X-0.5-21-550O	Chord + Branch-1	0.5	550
3	X-1.0-21-25O	Chord + Branch-2	1	25
4 (control)	X-1.0-21-550O	Chord + Branch-2	1	550

3 FE Model Validation

Commercial software, ANSYS v18.1, was used for all the FE models and analyses. The FE models were validated against experimental results from Fan and Packer's (2017) experimental study, and a sensitivity study is also performed.

3.1 *Connection Modeling*

Three-dimensional solid models of corresponding laboratory connections were created using ANSYS. For each model, the geometric volumes of chord and branch members were initially generated according to average measured member dimensions; then, the chord and branch were connected by fillet or PJP welds. The welds were modeled as prism volumes and the sizes of welds were based on experimental measurements. A sample FE model is shown in Fig. 2.

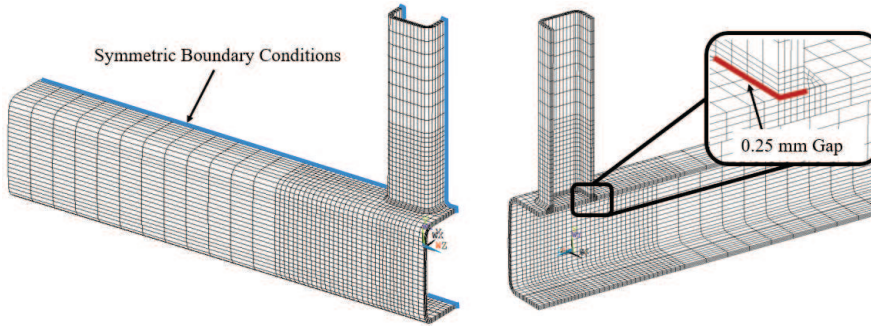

Figure 2. Sample connection model (Specimen 1)

Since the branch bottom surface and the chord top flange surface were not directly connected in actual experiments, a 0.25 mm gap was created in between the two members for each connection model. Considering that the two members may make contact at the gap location, contact pairs were generated between the two surfaces. Otherwise, connectivity was ensured between adjacent volumes.

A three-dimensional solid element defined by eight nodes, which is defined as SOLID185 in ANSYS element library, was selected for this non-linear analysis. The element has three translational degrees of freedom at each node and was applied to the FE models with full integration. The mesh of the solid model was generated by a semi-automated mapped mesh, where hexahedral elements were used. In order to reduce the number of elements generated in a model, the mesh density was adjusted throughout the model.

In FE models, an initial imperfection is recommended for elements in compression by CSA S16-19 (CSA 2019), as a bow-out imperfection, with the maximum permissible tolerance as the initial deformation. A bulge of $0.01h_0$ at the mid-height of the chord web was therefore introduced in the connection models as an initial imperfection, described by a sinusoidal function.

3.2 *Material Modeling*

Chord material properties were obtained from tensile coupon tests in the form of engineering stress-strain relationships. The results were then converted into true stress-strain relationships for the purpose of FE modeling input. The conversion was performed based on the recommendation of Callister (2007), and the converted true stress-strain curve is plotted in Fig. 3, where E is Young's Modulus, f_y is yield stress, f_u is ultimate stress, and ε_{rup} is rupture strain. Based on the converted results, a multilinear stress-strain curve was input into the FE models.

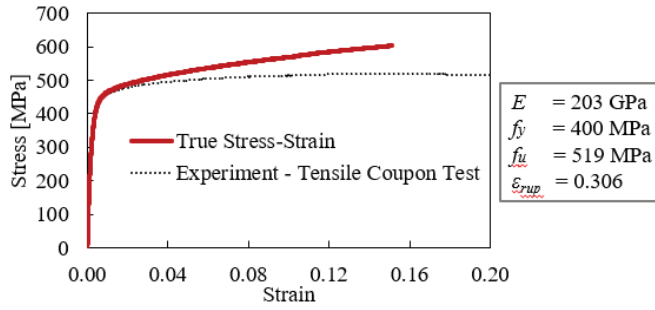

Figure 3. Representative tensile coupon test result and true stress-strain curve

Since failure occurred in the chord member (i.e., in the flanges or sidewalls) in Fan and Packer's (2017) experiments, the branch member and welds are not critical. Therefore, the chord material properties were also used for the branch and welds in the FE models.

3.3 *Boundary Conditions*

Since the connections are symmetric about the plane formed by the centerlines of the chord and the branch members, only half of the connection is modeled, and symmetrical boundary conditions are defined at the planes of symmetry. The symmetry boundary condition could significantly reduce the total number of elements used in analysis.

As there was no lateral restraint to the test specimen in the experiments, the bottom of the connection and the pedestal was a compression-only contact where the lateral restraint was provided by static friction. For contact between the chord and pedestal, the contact condition was analyzed as a surface-to-surface contact problem, with the contact stiffness set to default. The pedestal was modeled as a rigid surface, with all nodes fixed in all directions. Then, a rigid-flexible contact pair was created between the pedestal and the bottom surface of the chord member.

3.4 *Sensitivity Study*

Three major parameters affect the results of these FE models: (i) coefficient of friction at the pedestal, (ii) number of layers of elements through the thickness of the chord, and (iii) element density. The sensitivity study on Specimen 3 is presented in this paper. Once the combination of parameters was determined, the same parameters were applied to other specimens to demonstrate the accuracy of the choice.

The coefficient of friction between the pedestal and the chord was varied from 0.1 to 0.7, with an increment of 0.1. A relatively small coefficient is preferable to account for the fact that the contact surface between the specimen and the pedestal is relatively smooth (Fan and Packer 2017).

For FE models with hexahedral elements, the shape of the elements in the connection region was initially assumed to be cubic, with a general element size determined by the number of element layers through the chord thickness (thickness / number of layers). To study this effect, the number of layers was varied from two to five with an increment of one.

When the elements are approximately cubic the aspect ratio of the elements is 1.0, which corresponds to a scale factor of 1.0. The scale factor can be adjusted in any direction except the through-thickness direction. Once the scale factor in the other directions increases, the corresponding element aspect ratio increases by the same scale and the total number of elements decreases, which reduces the computational time.

By performing a sensitivity study, the parameters chosen were: 0.3 for coefficient of friction, four as the number of layers through the chord thickness, and 2.5 as a scale factor. Results for all specimens with the chosen combination of parameters are plotted in Fig. 4. The deformed shape and stress distribution of the Specimen 3 model, compared to the actual specimen photo, are shown in Fig. 5.

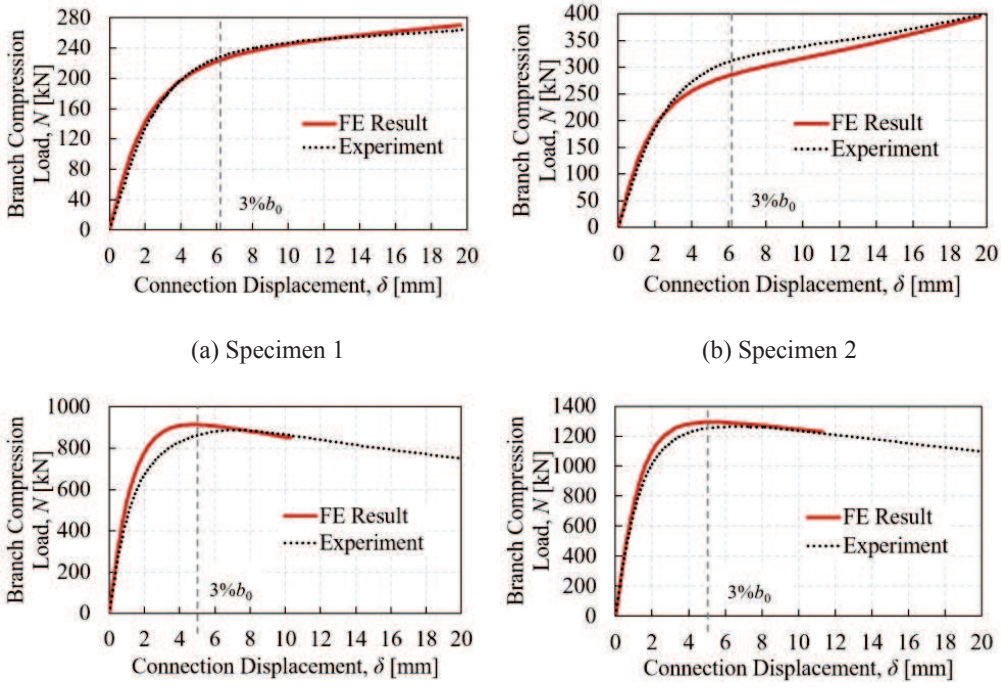

(a) Specimen 1

(b) Specimen 2

(c) Specimen 3

(d) Specimen 4

Figure 4. Experimental and FE results – load-displacement curves

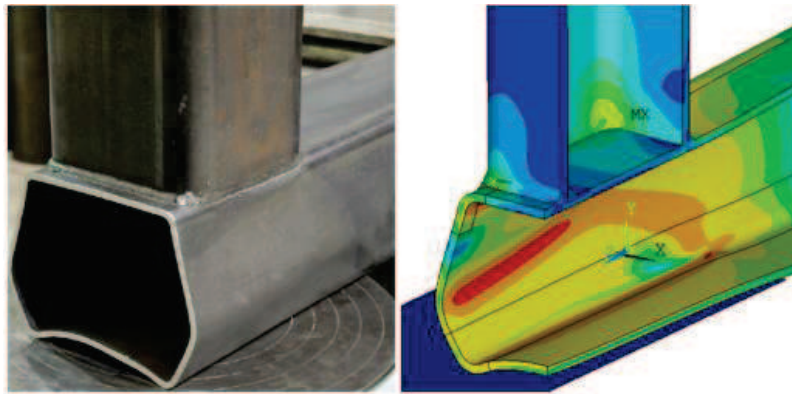

Figure 5. FE Model – Deformed Shape and Stress Distribution (Specimen 3)

4 Parametric Study

Using the validated FE models, a parametric study of longitudinally offset X-connections was performed. Instead of T-shaped connections, the parametric study focuses on X-shaped connections, which are more commonly used in actual design practice.

Rather than commercially available RHS members adhering to various standards, all RHS members used in this study are hypothetical RHS members, which are defined to fulfil the desired parameters. All the chord members in this study have the same width and height of 200 mm, while other chord dimensions and branch dimensions are varied according to other parameters of interest, e.g. β, 2γ, and e. The corner radii of the cold-formed cross sections were defined as t_0 and $2t_0$ for the chord inner and outer corner radius, respectively. For the branch members, thicknesses were used to ensure that the branches were non-critical.

Typical FE models used for the parametric study are shown in Fig. 6. These X-shaped models are adapted from the validated T-shaped models. For X-shaped connections, the chord is vertically symmetrical about its mid-height, so a plane of symmetry is generated at the chord mid-height. Other boundary conditions are the same as the validated T-shaped model, as well as the load application. Meanwhile, the material properties are the same as that used for validation.

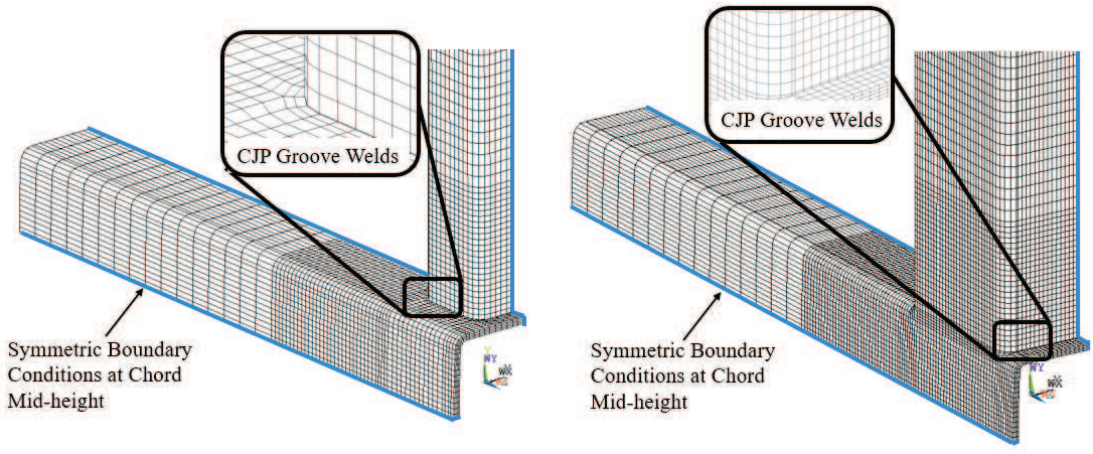

Figure 6. Typical connection models for parametric study

The welds in this parametric study were assumed to be complete joint penetration (CJP) groove welds, so the weld does not extend beyond the branch. In the FE models, the branches were connected to the chord without gaps. Details are shown in Fig. 6.

Considering the limits of validity of CIDECT Design Guide No.3 (Packer et al. 2009), the parameters were varied as follows: 2γ = 10, 15, 20, 25, 30, 35; β = 0.25, 0.5, 0.75, 1.0; and e = $0.1b_0$, $0.25b_0$, $0.5b_0$, $0.75b_0$, $1.0b_0$. Among all the combinations, connections of β = 0.75 with 2γ = 10 or 15 were excluded from the study. Meanwhile, for each valid 2γ and β combination, a control specimen was analyzed with the branches located midway along the chord and with end distances of $e = 3b_0$. Thus, a total of 132 analyses were performed in the parametric study.

4.1 *Effect of e*

The results are plotted in Fig. 7, with all the axes normalized. The horizontal axis is e/b_0, and the vertical axis is $N/N_{e,\,max}$ (where N is the connection strength for each connection, and $N_{e,\,max}$ is the full connection strength with $e = 3b_0$). Since the parametric study is performed for four different β values (0.25, 0.5, 0.75, 1.0), the results for each β are plotted separately. In Fig. 7, the results are plotted regardless of 2γ. The vertical dashed lines in Fig. 7 represent the minimum end distance of

$e_{min} = b_0\sqrt{1-\beta}$ for corresponding β, required by AISC 360-16 (AISC 2016) as derived by Fan and Packer (2017). Fig. 7 confirms that this rule (for minimal connection strength reduction), based solely on yield-line mechanisms in the chord face, is valid for β up to approximately 0.75.

As expected, it is observed that the connection strength decreases as the end distance decreases. According to the results, the strength reduction at $e = 1.0b_0$ is negligible, where the difference is generally less than 1%; meanwhile, the strength reduction at $e = 0.75b_0$ is also very small, being generally less than 2%. This is consistent with the experimental results by Fan and Packer (2017) which all had β = 0.5. When $e < 0.75b_0$, the strength reduction becomes more significant as e decreases. Considering the accuracy of design, it is acceptable to assume that the connection has full strength with a distance from a branch to an open chord end of $e \geq 0.75b_0$.

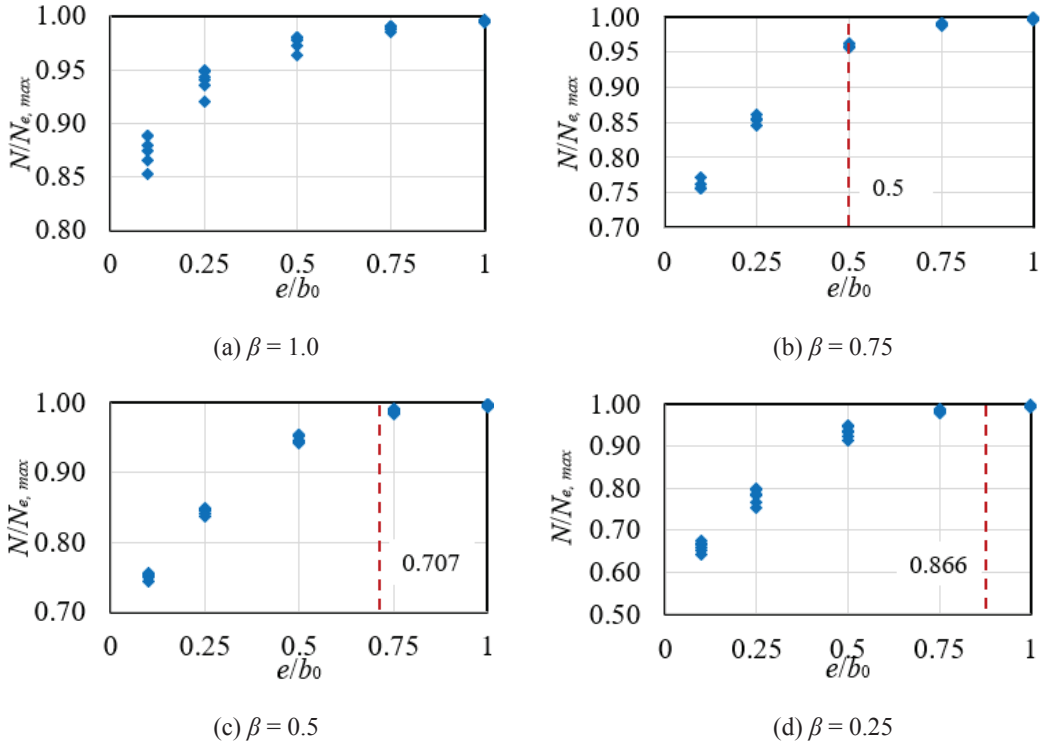

(a) $\beta = 1.0$ (b) $\beta = 0.75$

(c) $\beta = 0.5$ (d) $\beta = 0.25$

Figure 7. Connection strength vs. end distance

4.2 *Effect of β*

With the same e/b_0, the connection strength reduction varies with β. Generally, at the same e/b_0, as β decreases, $N/N_{e,\,max}$ also tends to decrease. The trend becomes more obvious as e/b_0 is smaller. The minimum $N/N_{e,\,max}$ values (for $e = 0.1b_0$) corresponding to $\beta = 0.25$, 0.5, 0.75, and 1.0 are 0.630, 0.744, 0.757, and 0.865, respectively, which are also plotted in Fig. 8.

In Fig. 8, a linear regression was performed to fit the linear relation between $N/N_{e,\,max}$ and β, which gives the dashed line in Fig. 8. For safe use in design, the linear curve was adjusted to the solid line in Fig. 8, which is a lower bound.

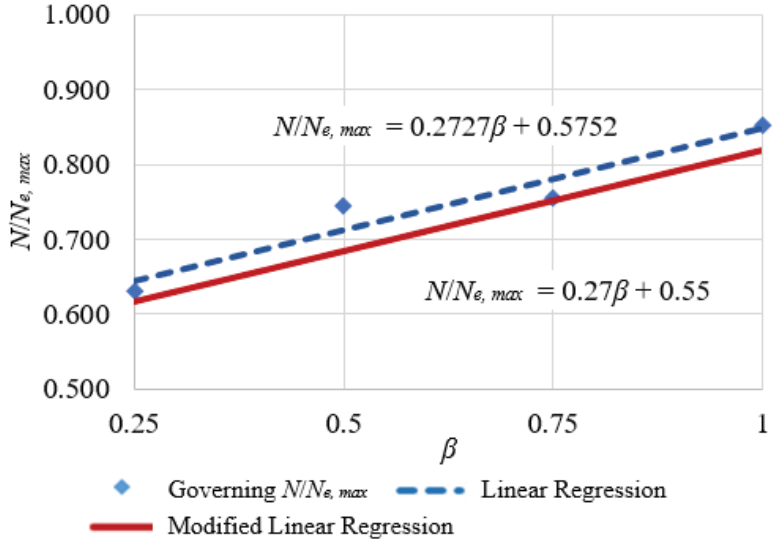

Figure 8. Linear regression of $N/N_{e,\,max}$ vs. β, for minimal e ($0.1b_0$)

5 Conclusions and Recommendations

Based on previous experimental tests of longitudinally offset RHS X-connections, FE models are built and validated against the experimental results with ANSYS. Using the validated FE models, a parametric study is performed on such type of connections.

It can be concluded that, for RHS X-connections with branches in axial compression and near an open chord end, a minimum end distance of $0.75b_0$ is required if the strength of the connection is not to be compromised. If the end distance is less than $0.75b_0$, the regular connection strength could be reduced using the factor: $N/N_{e,\,max} = 0.27\beta + 0.55$, where $0.25 \leq \beta \leq 1.0$. It should also be noted that the largest reduction in connection strength, for even very small end distances, is to 60% of the regular connection strength (remote from a chord open end).

Acknowledgments

Financial support for this project was provided by the Natural Sciences and Engineering Research Council of Canada (NSERC).

References

AISC, *ANSI/AISC 360-16, Specification for Structural Steel Buildings,* American Institute of Steel Construction, Chicago, 2016.

Callister, W. D., *Material science and engineering: an introduction*, 7th. ed., John Wiley & Sons. Inc., NJ, USA, 2007.

CEN, *EN 1993-1-8, Eurocode 3: Design of Steel Structures – Part 1-8: Design of Joints*, European Committee for Standardization, Brussels, 2005.

CEN, *prEN 1993-1-8, Eurocode 3: Design of Steel Structures – Part 1-8: Design of Joints*, European Committee for Standardization, Brussels, 2018.

CSA, *CSA S16-19, Design of steel structures*, Canadian Standards Association, Toronto, Canada, 2019.

Fan, Y. and Packer, J. A., RHS-to-RHS Axially Loaded X-Connections Near an Open Chord End, *Can. J. Civ. Eng*. 44, 881-892, 2017.

Packer, J.A., Wardenier, J., Zhao, X.-L., van der Vegte, G.J. and Kurobane, Y., *CIDECT Design Guide No.3, Design Guide for Rectangular Hollow Section (RHS) Joints under Predominantly Static Loading*, 2nd Ed., CIDECT, Geneva, 2009.